Evolution of magnetism of Cr nanoclusters on Au(111): First-principles electronic structure calculations

H. J. Gotsis and Nicholas Kioussis
Department of Physics, California State University Northridge, Northridge, California 91330-8268, USA

D. A. Papaconstantopoulos
Center for Computational Materials Science, Naval Research Laboratory, Washington D.C. 20375, USA
and School of Computational Sciences, George Mason University, Fairfax, Virginia 22030, USA
(Received 13 September 2005; published 31 January 2006)

We have carried out collinear and noncollinear electronic structure calculations to investigate the structural, electronic, and magnetic properties of isolated Cr atoms, dimers, and compact trimers. We find that the Cr monomer prefers to adsorb on the fcc hollow site with a binding energy of 3.13 eV and a magnetic moment of $3.93\mu_B$. The calculated Kondo temperature of 0.7 K for the monomer is consistent with the lack of a Kondo peak in scanning tunneling microscopy (STM) experiments at 7 K. The compact Cr dimer orders antiferromagnetically and its bond length contracts to 1.72 Å close to the value for the free-standing Cr dimer. The very low magnetic moment of $0.005\mu_B$ for the Cr atoms in the dimer is due to the strong *d-d* hybridization between the Cr adatoms. Thus, these calculations reveal that the absence of the Kondo effect observed in STM experiments is due to the small local moments rather than the Kondo quenching of the local moments suggested experimentally. The Cr compact trimer exhibits noncollinear coplanar magnetism with vanishing net magnetic moment in agreement with experiment.

DOI: 10.1103/PhysRevB.73.014436 PACS number(s): 75.75.+a, 75.70.Rf, 75.20.Hr

I. INTRODUCTION

The study of magnetism at the nanoscopic scale is a major research activity in condensed matter physics. Nanomagnetism is a highly demanding fundamental problem as well as important for applications in high density recording media and memory devices. A particularly attractive feature of these systems is the strong sensitivity of their electronic and magnetic properties to the geometrical and chemical environment of the atoms. Consequently, numerous experimental studies have been concerned with the production and characterization of a large variety of nanometer scale magnetic materials involving transition metals and noble metals in different structural arrangements.[1]

Magnetic transition-metal nanostructures on nonmagnetic substrates have attracted recently large attention due to their unusual magnetic properties.[2,3] The supported clusters experience both the reduction of the local coordination number, as in free clusters, as well as the interactions with the electronic degrees of freedom of the substrate, as in embedded clusters, which may lead to the Kondo effect.[4] The complex magnetic behavior is usually associated with the competition of several interactions, such as interatomic exchange and bonding interactions, the Kondo effect, and in some cases noncollinear effects, which can give rise to several metastable states close in energy.[3,5,6] The ground state can, therefore, be easily tuned by an external action giving rise to the switching between different states.

Recent advances in scanning tunneling microscopy (STM) and the ability to build magnetic clusters with well-controlled interatomic distances on metal surfaces have opened the possibility of probing *local* interactions in magnetic nanostructures assembled atom by atom at surfaces.[7–9] STM is ideal for studying the low-energy structure near the Fermi energy (E_F) since it allows access to states both above and below E_F. Recent STM studies have investigated the interplay between magnetic and electronic phenomena in one-impurity,[7] two-impurity,[8] and more recently, in three-impurity[9] systems. Cr is unique among the transition-metal adatoms, because its half-filled valence configuration ($3d^5 4s^1$) yields both a large magnetic moment and strong interatomic bonding leading to magnetic frustration.[10,11] The STM spectra for Cr clusters supported on the Au(111) surface can be summarized as follows.[9] The lack of a Kondo peak for the single Cr atom was attributed to the fact that the Kondo temperature T_K is significantly less than the experimental temperature of 7 K. The featureless STM spectrum observed for the dimer[8] was suggested to be due to the strong antiferromagnetic coupling between the atoms, which in turn quench the Kondo effect. Interestingly, compact triangular Cr trimers [Cr atoms occupying nearest-neighbor sites on the (111) Au surface] exhibited two distinct classes of behavior. In the first state, they displayed a featureless STM spectrum, whereas in the second they displayed a narrow resonance at the Fermi energy. Trimers were reversibly transferred from one state to the other by very small shifts of one atom via tip manipulation. It was suggested that the two observed states correspond to equilateral and isosceles trimer configurations, with a net trimer magnetic moment of zero and nonzero, respectively.

On the theoretical side, *ab initio* electronic structure calculations have been employed to study the collinear magnetic properties of 3*d* adatoms and clusters on the (001) Ag (Refs. 2 and 12) and Cu (Ref. 13) surfaces and the (111) Cu (Ref. 14) surface. The magnetic properties of small *free*-standing chromium clusters have been investigated by *ab*

initio electronic structure calculations for collinear[10] and noncollinear[11] magnetic ordering and a wide range of cluster geometries and atomic configurations. Both these calculations show that the isosceles triangular structure is the ground-state configuration, and that the noncollinear spins induce only very small changes in the cluster's geometry relative to the collinear model. Recently, the magnetic properties of noncollinear structures of supported chromium clusters have been studied within the phenomenological Anderson,[15] Coqblin-Schrieffer,[16] and Heisenberg[17] models.

The purpose of this work is to provide a first-principles investigation of the structural, electronic, magnetic properties, and the relative site preference of the Cr monomers, dimers, and trimers adsorbed on the Au(111) surface. Even though the first-principles electronic structure calculations cannot account for the many-body resonance at E_F associated with the Kondo effect,[18] these calculations elucidate the origin in the electronic structure of the evolution of the magnetic properties (spin and orbital moments) with cluster size and atomic geometry, including the possibility of noncollinear magnetism. To the best of our knowledge, this is the first *ab initio* study of noncollinear magnetic ordering for supported equilateral triangular trimers.

The next section gives a brief description of the theoretical method used in our study. In Sec. III we present the results of the electronic structure and the magnetic properties of the various Cr adatom configurations. Finally, we give a brief summary in Sec. IV.

II. THEORETICAL METHOD

The spin-polarized electronic structure calculations were done using the projector augmented-wave (PAW) method,[19] as implemented in the VASP code.[20] For the exchange-correlation potential we used the local spin-density approximation functional of Perdew and Wang.[21] An energy cutoff of 260 eV was used for the plane-wave expansion with the augmentation charge cutoff increased to 1040 eV.

To model the Au(111) surface, we adopt the slab supercell approach, where the slab consists of five gold layers with four atoms per layer for the monomers and nine atoms per layer for the dimers and the triangular trimers. A vacuum space corresponding to four Au layers is used to separate the central slab and its periodic images. The Brillouin zone integration was performed on a Monkhorst-Pack $7\times7\times1$ k-point mesh with a Methfessel-Paxton[22] smearing of 0.2 eV. The calculations have been performed allowing relaxation of the top three gold layers with the bottom two constrained at the bulk geometry, with the calculated equilibrium lattice constant of 4.063 Å compared to the experimental value of $a=4.08$ Å. Forces on the ions are calculated through the Hellmann-Feynman theorem as the partial derivatives of the free energy with respect to the atomic position, including the Harris-Foulkes[23]-like correction to forces. This calculation of the forces allows a geometry optimization using the quasi-Newton scheme.[24] Iterative relaxation of atomic positions was stopped when the change in total energy between successive steps was less than 0.001 eV. With this criterion, forces on the atoms were generally less than 0.1 eV/Å with lateral forces on chromium and gold surface layer atoms negligible. The geometry optimization was performed together with the spin-polarized electronic structure calculations. The mass-velocity and Darwin correction terms are incorporated into the PAW potentials and spin-orbit relativistic effects are included self-consistently. While the spin-orbit interaction determines the magnetocrystalline anisotropy energy, it does not influence the size of the magnetic moments, presented here, in a significant way. Noncollinear magnetic structures can be treated at various levels of sophistication[25] and the PAW approach allows for a fully unconstrained vector-field description of noncollinear magnetism.[26]

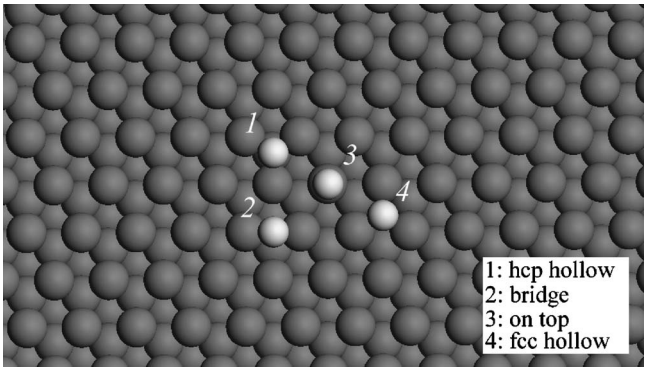

FIG. 1. Sketch of the Au(111) surface and its high-symmetry adsorption sites.

III. RESULTS AND DISCUSSION

A. Monomers

In order to understand the adsorption behavior of the Cr monomer, we have calculated the binding energies, magnetic moments, and surface-atom distances for Cr adsorbed at four principal adsorption sites of the Au(111) surface shown in Fig. 1. These include on top sites, bridging sites between two atoms, and hcp and fcc hollow sites between three atoms. In the hcp (fcc) hollow site there is an atom directly beneath the second (third) layer. The adsorption energies have been calculated using

$$E_{bind} = E(\text{Pure} + \text{Cr}) - E(\text{Pure}) - E(\text{Cr}), \qquad (1)$$

where E(Pure+Cr) represents the total energy of the slab with the Cr adatom, E(Pure) represents the total energy of the pure (clean) surface and E(Cr) represents the total energy of an isolated Cr atom. An isolated Cr atom was approximated by a single atom in a simple cubic cell with lattice constant of 15 Å. Its total energy was then calculated using only the Γ point in the Brillouin zone integration. The binding energies E_{bind}, the spin magnetic moment, and the Cr-surface distance for the four adsorption sites are listed in Table I. We find that the preferred adsorption site is the fcc hollow, with a binding energy of −3.129 eV and a spin moment of $3.93\mu_B$. Furthermore, the binding energy on the hcp hollow site of −3.104 eV is very close to that of the fcc hollow site, suggesting that the chromium binds at high co-

TABLE I. Calculated binding energies E_{bind}, spin magnetic moments, and Cr-surface distances $d_{Cr\text{-}Au}$ for Cr adatoms adsorbed on different sites on the Au(111) surface.

Adsorption site	E_{bind} (eV)	Magnetization (μ_B)	$d_{Cr\text{-}Au}$ (Å)
On top	−2.334	4.13	2.426
fcc hollow	−3.129	3.93	1.931
Bridge	−3.046	3.93	1.993
hcp hollow	−3.104	3.94	1.937

ordination sites. The on top site is less favorable by about 0.8 eV and has the largest spin moment of $4.13\mu_B$. The value of the magnetic moment for the on top adsorption site is in good agreement with the calculated value of $4.3\mu_B$ for a Cr adatom adsorbed on the top site on the Au(001) surface reported bu Cabria *et al.*[2] The larger value of the magnetic moment in Ref. 2 is due to the fact that lattice relaxations were neglected in these calculations. We find that, as expected, the spin moment is dominated by the contribution of the Cr *d*-electron states (the *s*- and *p*-derived contributions are less than 4% of the total). Moreover, the induced spin moments on the Au(111) surface are negligible. Note, that the trend of values of the height of the Cr adatom from the Au surface, $d_{Cr\text{-}Au}$, correlates well both with the trend of binding energies and the magnetic moments, i.e., the shorter $d_{Cr\text{-}Au}$ is associated with the largest binding energy and the smaller moment, due to the stronger hybridization of the 3*d* orbitals with the 6*s* conduction band of the Au substrate.

We have also carried out spin-polarized electronic structure calculations for the fcc hollow site with the spin-orbit coupling included self-consistently. In Table II we present the orbital and spin components of the magnetic moment for a single Cr adatom, where the spin- and orbital-quantization axis is chosen perpendicular to the surface. As expected, the orbital-moment values for the adatom are low, consistent with the zero orbital moment value for the isolated chromium atom. The S_z component of the moment is $3.903\mu_B$,

TABLE II. Calculated magnetic moments for a Cr adatom in a fcc hollow at the Au(111) surface. The orbital magnetic moments L_δ for $\delta=x,y,z$, the corresponding spin magnetic moments S_δ, and the total magnetic moment M are given in Bohr magnetons (μ_B).

L_x	L_y	L_z	S_x	S_y	S_z	M
−0.01	−0.01	−0.01	0.02	0.00	3.90	3.89

which is virtually identical to that from the calculation where the spin-orbit coupling was not included (Table I), indicating that the effect of the spin-orbit coupling is small.

In Fig. 2 we show the spin-polarized local density of states (DOS) of the Cr adatom on an fcc hollow site and the layer-resolved DOS in the first two top layers (surface S and subsurface S-1) of the five-layer Au(111) slab. The majority (minority) spin states are shown in the positive (negative) portion of each panel. The solid curves correspond to the spin-polarized DOS without spin-orbit coupling and the dashed curves denote the total DOS with spin-orbit coupling included. The Fermi energy, placed at 0 eV, lies in the 6*s* Au derived states region. The Cr adatom DOS for the majority (minority) spin state shows Lorentzian-shaped virtual states centered at E_d-E_F (E_d-E_F+U) $\sim$0.5 eV ($\sim$2.5 eV) below (above) the Fermi energy. This yields an intra-atomic Coulomb interaction U for the Cr adatom of about 3 eV. The majority spin virtual bound state has a half-width of $\Delta \sim 0.075$ eV, due to the hybridization of the adatom 3*d* with the 6*s* states of the Au host. In the Anderson model which describes the behavior of a paramagnetic impurity in a nonmagnetic metal host the Kondo temperature T_K can be calculated from[4]

$$k_B T_K \sim \sqrt{\frac{\Delta U}{2}} e^{-\pi/2\Delta U|E_d-E_F||E_d-E_F+U|}. \quad (2)$$

Thus, we find that the single Cr-adatom Kondo temperature is about $T_K \approx 0.7$ K, which is much less than the experimental temperature of 7 K, consistent with the featureless STM

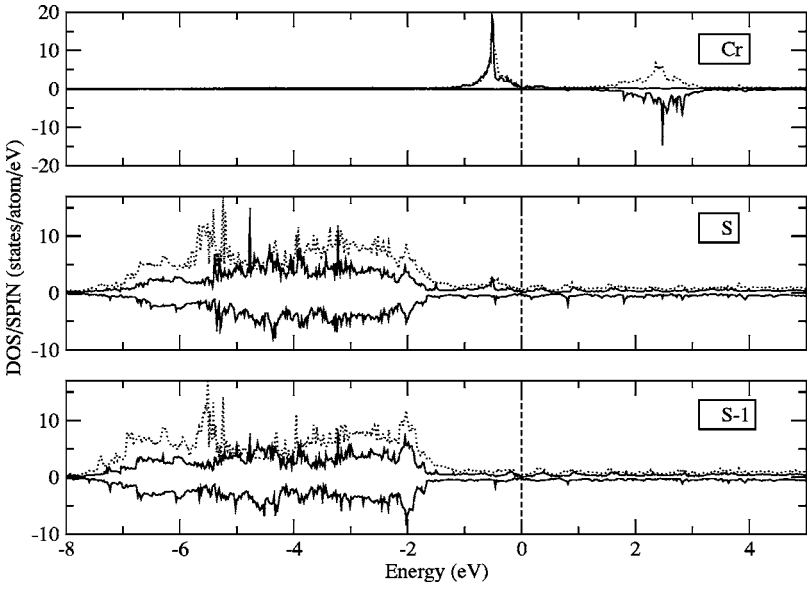

FIG. 2. Spin-projected local DOS of a Cr adatom on a fcc hollow site and the corresponding layer-resolved DOS of the Au(111) surface (S) and subsurface (S-1) (solid curves, respectively. The dotted curves denote the total DOS when including the spin-orbit coupling. The Fermi level is placed at 0 eV (dashed line).

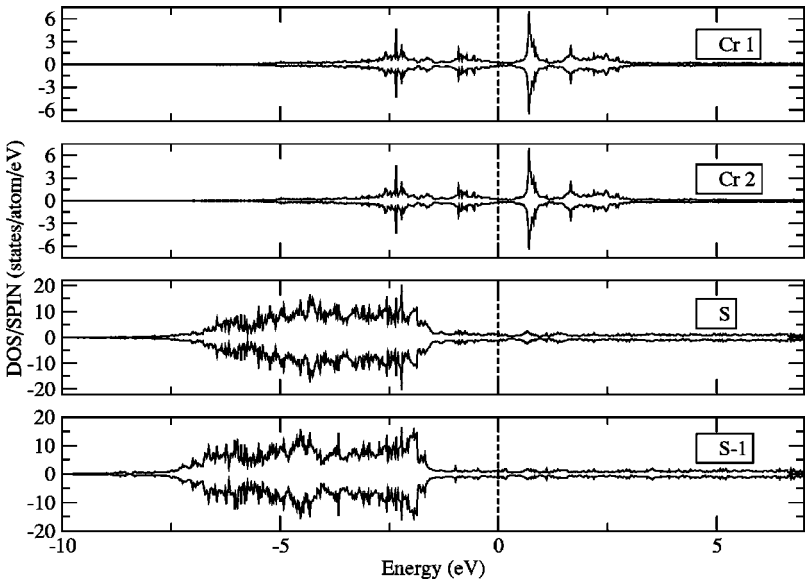

FIG. 3. Spin-projected local DOS of the Cr dimer and the corresponding layer-resolved DOS of the Au(111) slab. The Fermi level is placed at 0 eV.

spectrum observed experimentally. It should be emphasized that the fitting of the parameters of an Anderson model to the results of a local density approximation calculation can provide only a rough estimate of the Kondo temperature.

B. Dimers

In order to study the evolution in electronic and magnetic properties as two Cr monomers are merged into a single magnetic molecule on Au(111), we have performed structural energy minimization for a Cr dimer deposited on fcc hollow sites with an unrelaxed dimer bond length of 2.87 Å. As expected, the ground state of the cluster was found to be antiferromagnetic, reminiscent of the bulk. Interestingly, after the relaxation of the chromium adatoms and the outermost surface layers, the dimer bond length contracts to 1.72 Å, which is consistent with the value of 1.68 Å for the free Cr dimer reported by Cheng and Wang[10] and Bondybey and English.[27] At equilibrium, the two Cr atoms occupy a hcp and a fcc hollow sites, respectively, with moments of $0.005\mu_B$ and $-0.005\mu_B$ for each adatom, respectively. This is in agreement with the value of $0\mu_B$ per atom in the case of the free dimer.[10,11] For the dimer binding energy, a generalization of Eq. (1) gives the value of −3.65 eV/adatom which is lower than the corresponding value of −2.28 eV/atom for the free-standing dimer.[10] The low magnetic moment and higher binding energy is due to the strong 3*d*-3*d* hybridization between the Cr adatoms in the dimer which results to a very stable electronic structure.[10] More specifically, the Cr dimer has a unique electronic configuration (closed-shell system), where the *bonding* orbitals formed by the 3*d* orbitals of the Cr atoms are almost completely filled. This electronic configuration results in a strong 3*d*-3*d* hybridization, as can be seen in the spin-projected density of states in Fig. 3, which in turn lowers the total energy and results in a strong direct antiferromagnetic exchange interaction between the Cr atoms and an unusually short dimer bond length. Thus, these calculations suggest that the absence of the Kondo effect for the Cr dimer with a bond length of 1.72 Å is due to the vanishing of the magnetic moment of the adatom, rather than the experimentally suggested[9] picture of nonzero Cr magnetic moments which are locked in a singlet due to the antiferromagnetic exchange interactions.

The spin-polarized (without spin-orbit coupling) local density of states DOS of the Cr adatoms in the dimer and the layer-resolved DOS in the first two top layers of the Au(111) slab are shown in Fig. 3. The two uppermost panels show the DOS of the two Cr monomers where one can clearly see the strong 3*d*-3*d* hybridization. The majority (minority) spin states are shown in the positive (negative) portion of each panel. For both Cr1 and Cr2 adatoms, the two spin components are the same, and each adatom is accordingly nonmagnetic. This picture is consistent with the values of the calculated magnetic moments. In general, there is an interplay between the *direct* exchange interaction between the spins of adatoms resulting from the hybridization of the Cr 3*d* orbitals and the *indirect* exchange interaction between the adatoms mediated through the substrate conduction electrons. The latter *s*-*d* exchange interaction between the 3*d* Cr orbitals and the substrate conduction electrons J_{sd}, is also responsible for the Kondo effect. For small separations between adatoms (as in our case), the direct exchange interaction dominates the magnetic interactions. On the other hand, if the two adatoms are placed sufficiently far apart, the indirect exchange interaction dominates, provided it is larger than the single-adatom Kondo temperature. In comparison with Fig. 2 we find a broadening of the Lorentzian-shaped virtual states and a shift of the *d*-orbital states away from the Fermi energy ($E_d - E_F \sim 2.3$ eV below E_F) compared to the Cr monomer case. This results in a strong hybridization between the chromium *d* and gold *d* bands. The exchange interaction J_{sd} between the localized Cr *d* orbitals and the conduction electrons of the Au substrate can be written in the form[4]

$$J_{sd} \sim \frac{2V_{sd}^2 U}{(E_d - E_F)(E_d + U_d - E_F)}, \tag{3}$$

where V_{sd} is the *d*-conduction electrons hybridization, which can be determined from the half-width, Δ, of the virtual state

TABLE III. Local spin moments of an equilateral Cr trimer, in a noncollinear magnetic configuration, deposited on the Au(111) surface. The magnetic moments and the modulus of the moments are given in Bohr magnetons (μ_B).

Cr site	S_x	S_y	S_z	Modulus
Cr1	−0.00	3.16	−0.00	3.16
Cr2	−2.74	−1.58	−0.00	3.16
Cr3	2.73	−1.58	−0.00	3.15

in the Anderson model, $\Delta = 2\pi|V_{sd}|^2\rho(E_F)$. Here, $\rho(E_F)$ is the substrate density of states at the Fermi energy. The shift of the d orbital states away from E_F for the Cr atom in the dimer leads to a further reduction in J_{sd} and hence, a further reduction of the Kondo temperature, T_K, for Cr dimers. Thus, our results suggest that the strong direct antiferromagnetic exchange interactions are responsible for the zero magnetic moment of the Cr atoms in the dimer.

C. Trimers

Our *ab initio* calculations for collinear antiferromagnetic ordering perpendicular to the surface failed to converge due to the magnetic frustration associated with the geometry of the equilateral trimer. On the other hand, we find that the compact Cr trimer in the equilateral configuration displays coplanar noncollinear spin antiferromagnetic ordering due to the competition of the exchange interactions between the different atoms. The electronic and magnetic structures are investigated within noncollinear magnetism by considering each magnetic moment on each Cr atom as a vector. We have performed structural energy minimization for a Cr equilateral trimer originally deposited on fcc hollow sites with a bond length of 2.87 Å (nearest-neighbor sites). In the equilibrium configuration, the bond length contracts to 2.39 Å preserving the equilateral geometry. From Table III we observe that the angle between each pair of moments equals 120° and the total spin moment of the trimer is zero. The modulus of the moments on each atom of the trimer of $3.15\mu_B$ is comparable to the monomer values and remarkably enhanced relatively to the bulk spin moment value of approximately $0.5\mu_B$/atom[28] (Cr bulk has an antiferromagnetic ground state with a moment smaller than might be expected from its half-filled $3d$ shell, indicating its nearness to a magnetic instability).

Figure 4 shows the local DOS of the Cr adatoms and of the Au atoms in the surface. The DOS of Cr atoms are all the same due to the symmetric structure. With the atomic moments deviating from collinear alignment, the local spin projection is no longer a good quantum number specifying the electron states as spin-up and spin-down. However, due to the large magnetic moment, in the energy region below (above) the Fermi level there are preferentially states with a positive (negative) spin projection. The strong hybridization between the Cr d orbitals leads to a wider Cr bandwidth and the splitting of the Lorentzian-shaped virtual state for the monomer in Fig. 2.

It is known that, besides exchange, the spin-orbit coupling (SOC) can also be responsible for noncollinearity of the magnetic structure even if the SOC is very small in the $3d$ transition elements. Therefore, we carried out calculations that take account of both the noncollinearity of the magnetic moments and the SOC. One can see in Fig. 4 that the effect of SOC on the DOS of Cr atoms is small. In Table IV we list values of the orbital and spin components of the magnetic moments for the Cr trimer. The orbital moments are, in general, a factor of 2 larger than those for the monomer orbital (Table II), whereas the total magnetic moments M are smaller than the monomer case. Finally, the spin magnetic moments are very close to the values from the calculation where the SOC was not included, indicating that the magnetic (spin only) frustration is the main reason for the noncollinear structure formation in the trimer (Table III).

IV. CONCLUSION

In conclusion, we have carried out first-principles electronic structure calculations to study the structural, elec-

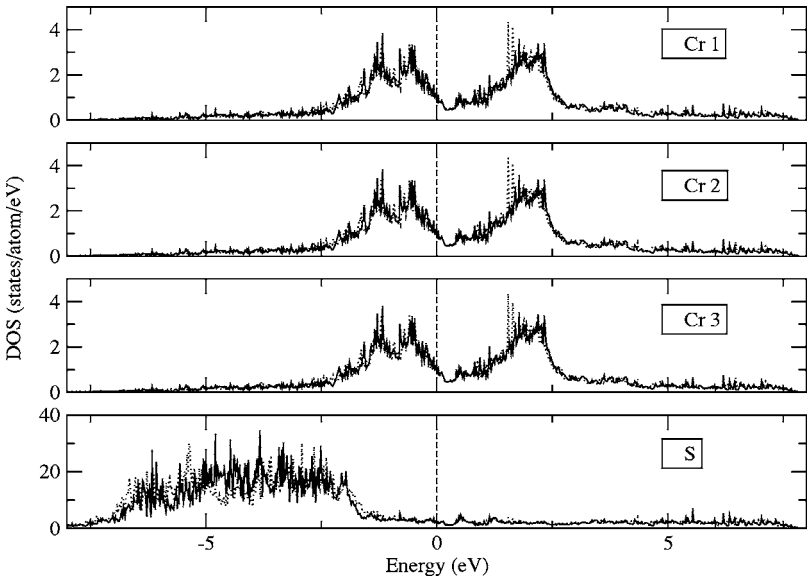

FIG. 4. Local DOS of the Cr trimer in a noncollinear configuration and the corresponding surface layer DOS of the Au(111) slab without spin-orbit coupling (solid curve). The dotted line denotes the total DOS when spin-orbit coupling is included. The Fermi level is set at 0 eV.

TABLE IV. Calculated magnetic moments of an equilateral Cr trimer, in a noncollinear magnetic configuration, at the Au(111) surface, with spin-orbit coupling included. The orbital magnetic moments L_δ for $\delta=x,y,z$, the corresponding spin magnetic moments S_δ, and the total magnetic moment M are given in Bohr magnetons (μ_B).

Cr site	L_x	L_y	L_z	S_x	S_y	S_z	M
Cr1	0.00	−0.03	0.02	−0.00	3.17	−0.00	3.17
Cr2	0.02	0.01	0.02	−2.75	−1.58	−0.00	3.17
Cr3	−0.02	0.01	0.02	2.74	−1.58	0.00	3.14

tronic, and magnetic properties of monomer, dimer, and trimer Cr clusters on the Au(111) surface. Our results show that the fcc hollow is the most favorable location for the single Cr adatom and has a binding energy of 3.3 eV and a magnetic moment of $3.93\mu_B$. The Cr DOS for the majority (minority) spin state shows Lorentzian-shaped virtual states centered at E_d-E_F (E_d-E_F+U) ~ 0.5 eV (~ 2.5 eV) below (above) the Fermi energy. The calculated single Cr Kondo temperature of 0.7 K is consistent with the lack of a Kondo effect at 7 K in STM experiments. The compact dimer is found to order antiferromagnetically, has a very short bond length of 1.72 Å, and a very low magnetic moment of $0.005\mu_B$. This is due to the strong *d-d* hybridization between the Cr atoms. Thus, these calculations reveal that the lack of the Kondo effect observed in STM experiments is due to the small Cr magnetic moments rather than the Kondo suppression of the local moment, as has been suggested in the analysis of experiments. The results for the noncollinear triangular compact trimer predict that the net spin cluster magnetic moment is zero, consistent with the featureless spectrum of the STM study. Future work will be aimed at investigations of the linear trimer and isosceles triangle cases, as well as of collinear magnetism perpendicular to the surface.

ACKNOWLEDGMENTS

One of us (H.J.G.) would like to thank Gang Lu and N. C. Bacalis for useful conversations and advice. This work was supported in part by the NSF under Grant No. DMR-00116566 and the US Army under Grant Nos. AMSRD-45815-PH-H and W911NF-04-1-0058, respectively.

[1] See, e.g., *Nanoscale Materials*, edited by Prashant V. Kamat and Luis M. Liz Marzan (Kluwer, Dordrecht, 2002), and references therein.
[2] I. Cabria, B. Nonas, R. Zeller, and P. H. Dederichs, Phys. Rev. B **65**, 054414 (2002).
[3] F. J. Himpsel, J. E. Ortega, G. J. Mankey, and R. F. Willis, Adv. Phys. **47**, 511 (1998).
[4] A. C. Hewson, *The Kondo Problem to Heavy Fermions* (Cambridge University Press, Cambridge, 1993).
[5] S. Jing, S. Gider, K. Babcock, and D. D. Awschalom, Science **271**, 937 (1996).
[6] T. Oda, A. Pasquarello, and R. Car, Phys. Rev. Lett. **80**, 3622 (1998).
[7] H. C. Manoharan, C. P. Lutz, and D. W. Eigler, Nature (London) **403**, 512 (2000); V. Madhavan, W. Chen, T. Jamneala, M. F. Crommie, and N. S. Wingreen, Science **280**, 567 (1998); T. Jamneala, V. Madhavan, W. Chen, and M. F. Crommie, Phys. Rev. B **61**, 9990 (2000).
[8] W. Chen, T. Jamneala, V. Madhavan, and M. F. Crommie, Phys. Rev. B **60**, R8529 (1999); V. Madhavan, T. Jamneala, K. Nagaoka, W. Chen, J.-L. Li, S. G. Louie, and M. F. Crommie, *ibid.* **66**, 212411 (2002).
[9] T. Jamneala, V. Madhavan, and M. F. Crommie, Phys. Rev. Lett. **87**, 256804 (2001).
[10] H. Cheng and Lai-Sheng Wang, Phys. Rev. Lett. **77**, 51 (1996).
[11] C. Kohl and G. F. Bertsch, Phys. Rev. B **60**, 4205 (1999).
[12] B. Nonas, I. Cabria, R. Zeller, P. H. Dederichs, T. Huhne, and H. Ebert, Phys. Rev. Lett. **86**, 2146 (2001); B. Lazarovits, L. Szunyogh, and P. Weinberger, Phys. Rev. B **65**, 104441 (2002).
[13] J. Izquierdo, D. I. Bazhanov, A. Vega, V. S. Stepanyuk, and W. Hergert, Phys. Rev. B **63**, 140413(R) (2001); S. Pick, V. S. Stepanyuk, A. N. Baranov, W. Hergert, and P. Bruno, *ibid.* **68**, 104410 (2003).
[14] B. Lazarovits, L. Szunyogh, P. Weinberger, and B. Újfalussy, Phys. Rev. B **68**, 024433 (2003).
[15] S. Uzdin, V. Uzdin, and C. Demangeat, Europhys. Lett. **47**, 556 (1999); Surf. Sci. **482-485**, 965 (2001).
[16] Yu. B. Kudasov and V. M. Uzdin, Phys. Rev. Lett. **89**, 276802 (2002).
[17] V. V. Savkin, A. N. Rubtsov, M. I. Katsnelson, and A. I. Lichtenstein, Phys. Rev. Lett. **94**, 026402 (2005).
[18] *Electron Correlations and Materials Properties*, edited by A. Gonis, N. Kioussis, and M. Ciftan (Kluwer Academic/Plenum Publishers, New York, 1998).
[19] G. Kresse and D. Joubert, Phys. Rev. B **59**, 1758 (1999).
[20] G. Kresse and J. Hafner, Phys. Rev. B **47**, 558 (1993); G. Kresse and J. Furthmuller, *ibid.* **54**, 11169 (1996); Comput. Mater. Sci. **6**, 15 (1996).
[21] J. P. Perdew and Y. Wang, Phys. Rev. B **45**, 13244 (1992).
[22] M. Methfessel and A. T. Paxton, Phys. Rev. B **40**, 3616 (1989).
[23] J. Harris, Phys. Rev. B **31**, 1770 (1985); W. M. Foulkes and R. Haydock, *ibid.* **39**, 12520 (1989).
[24] P. Pulay, Chem. Phys. Lett. **73**, 393 (1980).
[25] J. Kübler, K. H. Höck, and J. Sticht, J. Appl. Phys. **63**, 3482 (1988); R. Lorenz, J. Hafner, S. S. Jaswal, and D. J. Sellmyer, Phys. Rev. Lett. **74**, 3688 (1995); L. Nordström and D. J. Singh, *ibid.* **76**, 4420 (1996).
[26] D. Hobbs, G. Kresse, and J. Hafner, Phys. Rev. B **62**, 11556 (2000).
[27] V. E. Bondybey and J. H. English, Chem. Phys. Lett. **94**, 443 (1983).
[28] E. Fawcett, Rev. Mod. Phys. **60**, 209 (1988).